Supporting Information

A dual-mode colorimetric sensor based on copper nanoparticles for the detection of mercury-(II) ions

Qiang Li,[a,b] Feng Wu,[b] Mao Mao,[b,c] Xiang Ji, [b,c] Luyao Wei,[d] Jieying Li,[a,b] and Lan Ma [b,d]*

[a]*Department of Chemistry, Tsinghua University, Beijing 100084, P. R. China*

[b]*State Key Laboratory of Chemical Oncogenomics, Division of Life Science and Health, The Graduate School at Shenzhen, Tsinghua University, Shenzhen 518055, P. R. China*

[c]*School of Life Science, Tsinghua University, Beijing 100084, P. R. China*

[d]*Tsinghua-Berkeley Shenzhen Institute, Tsinghua University, Beijing, 100084, P.R. China.*

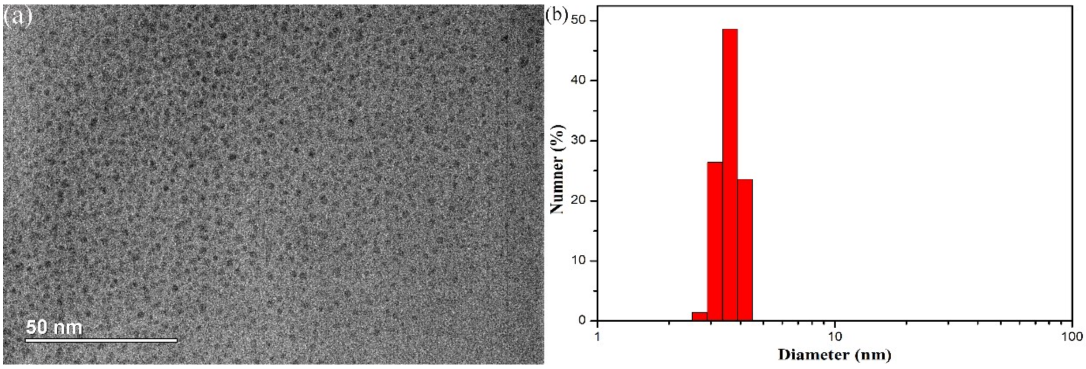

Figure S1. (a) TEM image and (b) DLS data of the citrate-capped Cu NPs. (citrate-capped Cu NPs dispersed in water)

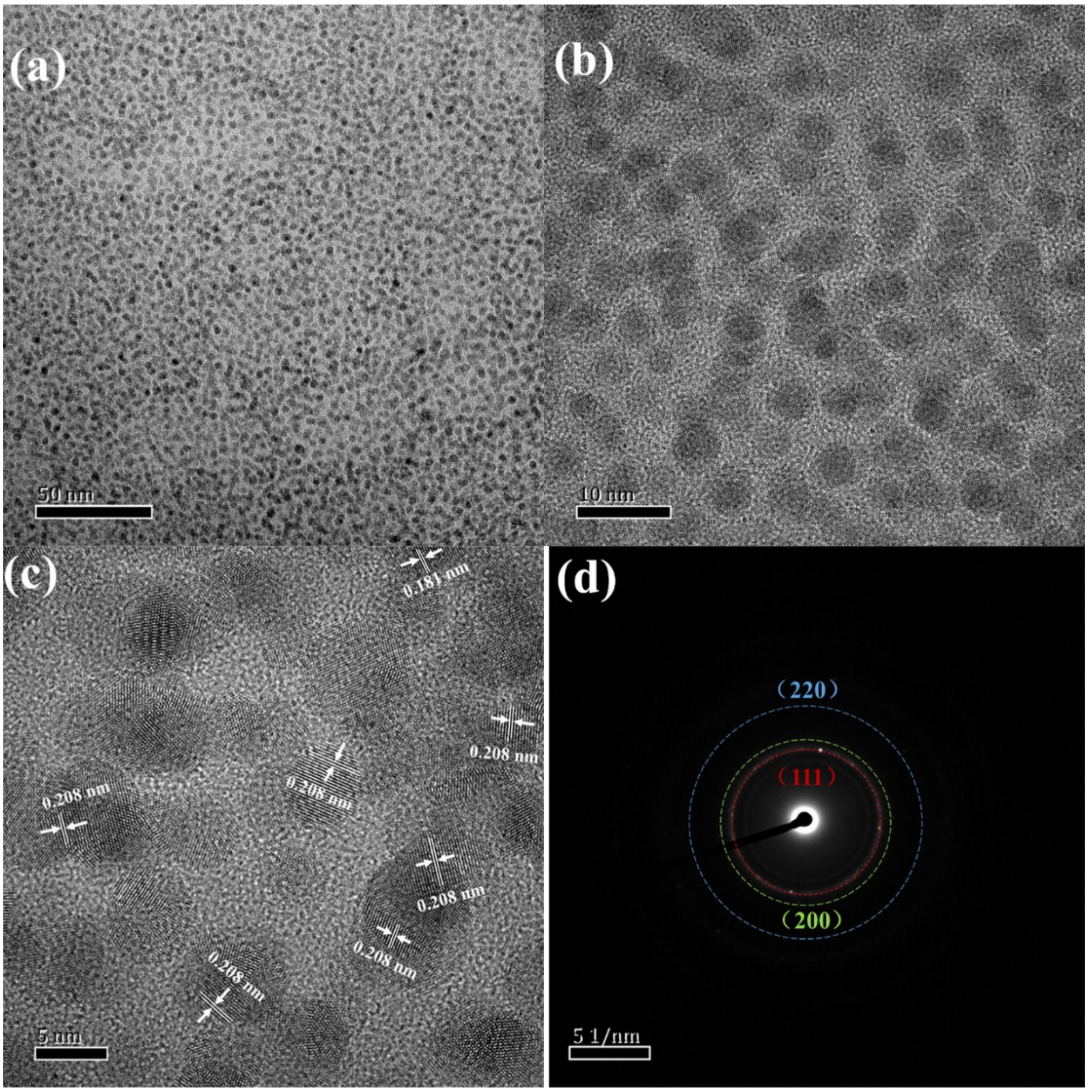

Figure S2. (a)~(c) TEM image and (d) SAED image of citrate-capped Cu NPs. (citrate-capped Cu NPs dispersed in ethanol)

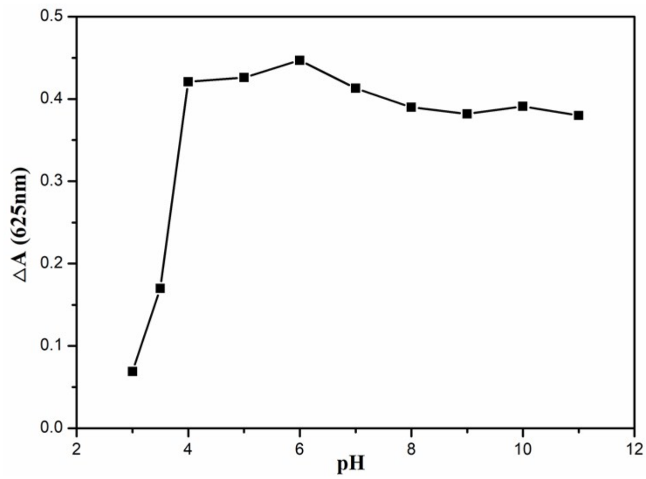

Figure S3. Effect of pH on ΔA. Reaction conditions: TMB,0.743 mM; H_2O_2, 0.177 M; citrate-capped Cu NPs, 100 µl; incubation temperature, 25 ℃; incubation time, 10 min; Hg^{2+} (10 µM), 500 µl; NaAc buffer, 2 ml.

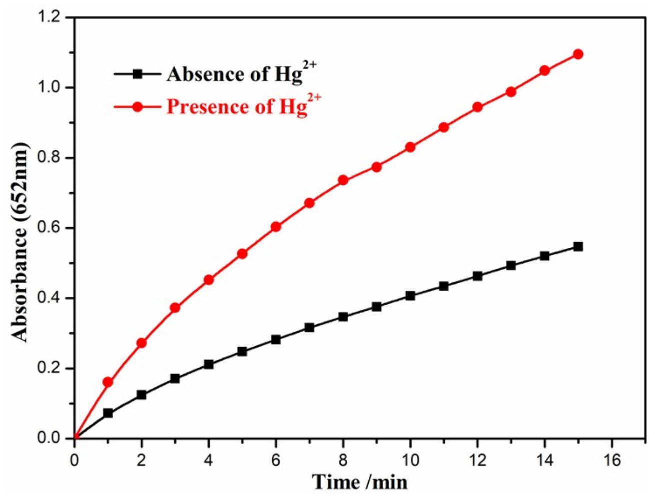

Figure S4. Effect of the incubation time on A_{652}. Reaction conditions: TMB,0.743 mM; H_2O_2, 0.177 M; citrate-capped Cu NPs, 100 µl; incubation temperature, 25 ℃; pH, 4.0; Hg^{2+} (10 µM), 500µl; NaAc buffer, 2ml.

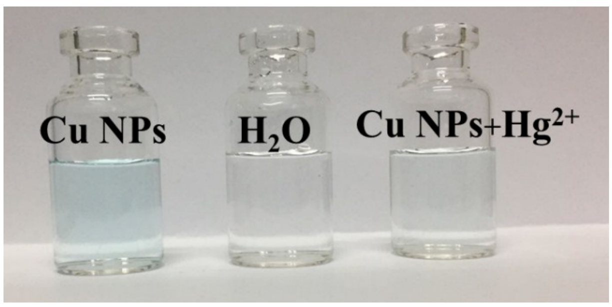

Figure S5. The photographs of citrate-capped Cu NPs before and after treatment with Hg^{2+}

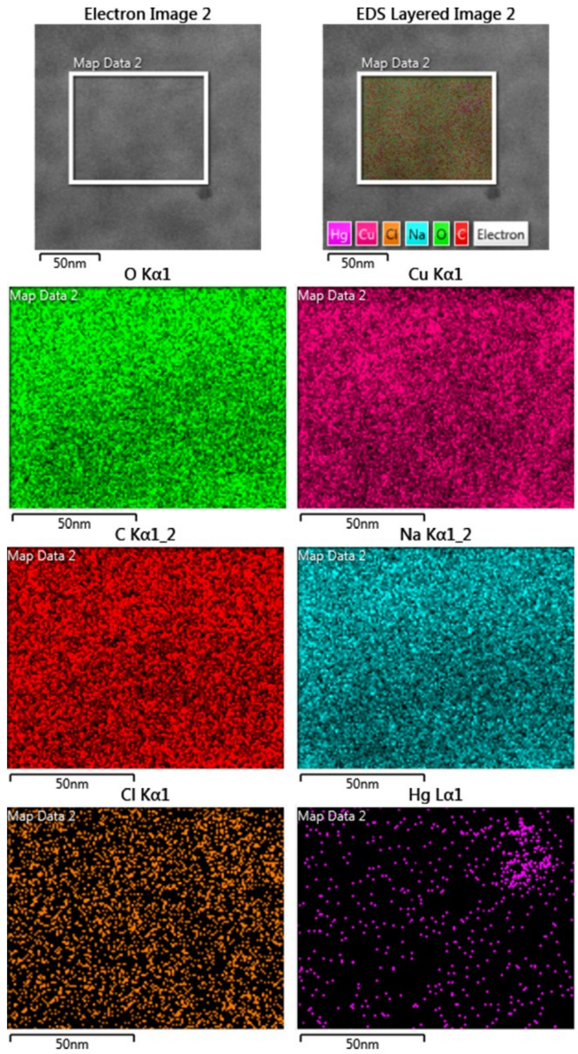

Figure S6. A series of TEM X-ray maps from citrate-capped Cu NPs after addition of Hg^{2+}.

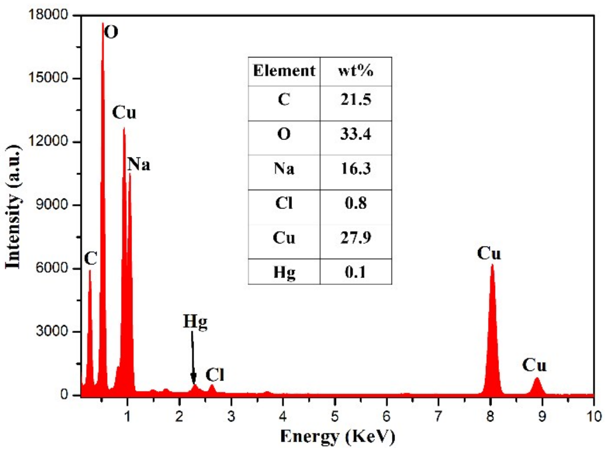

Figure S7. A series of TEM X-ray maps from citrate-capped Cu NPs after addition of Hg^{2+}.

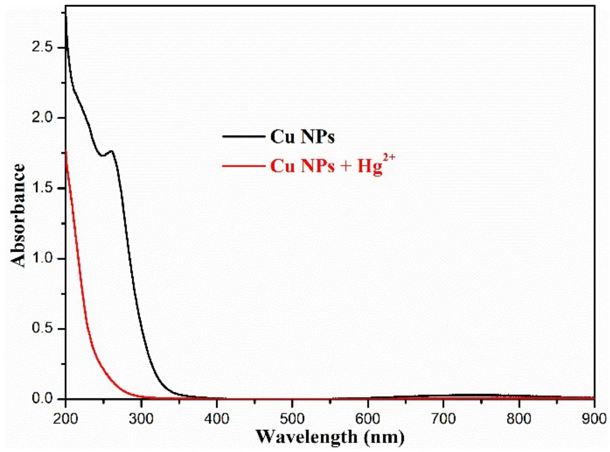

Figure S8. UV-Vis absorption spectra of citrate-capped Cu NPs with and without Hg^{2+}

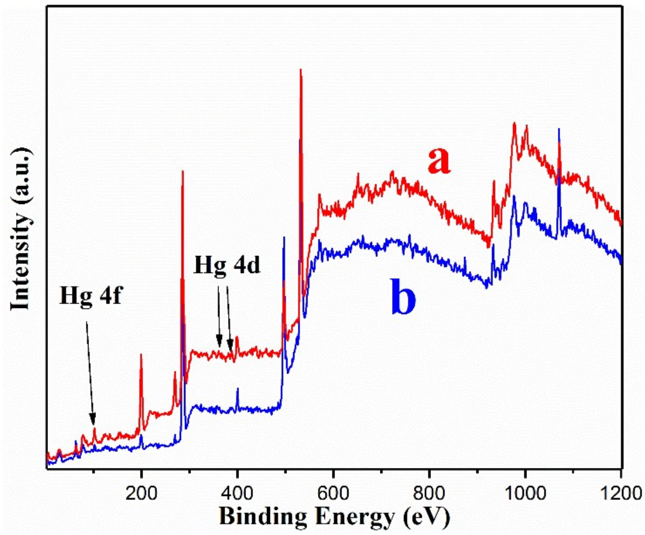

Figure S9. XPS spectra of citrate-capped Cu NPs (a) before and (b) after treatment with Hg^{2+}

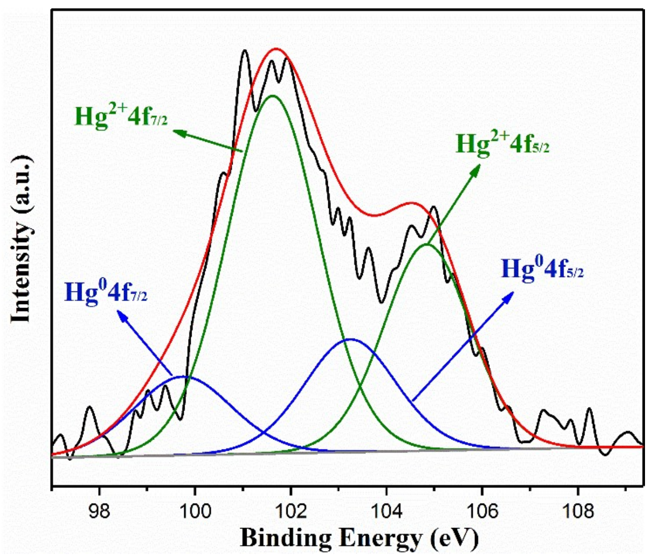

Figure S10.Hg 4f XPS spectrum of the citrate-capped Cu NPs after treatment with Hg^{2+}

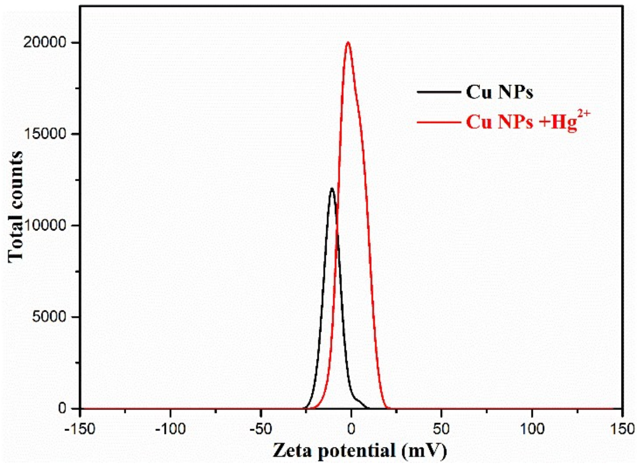

Figure S11. The apparent zeta potential curves of the citrate-capped Cu NPs in the absence and presence of Hg^{2+}

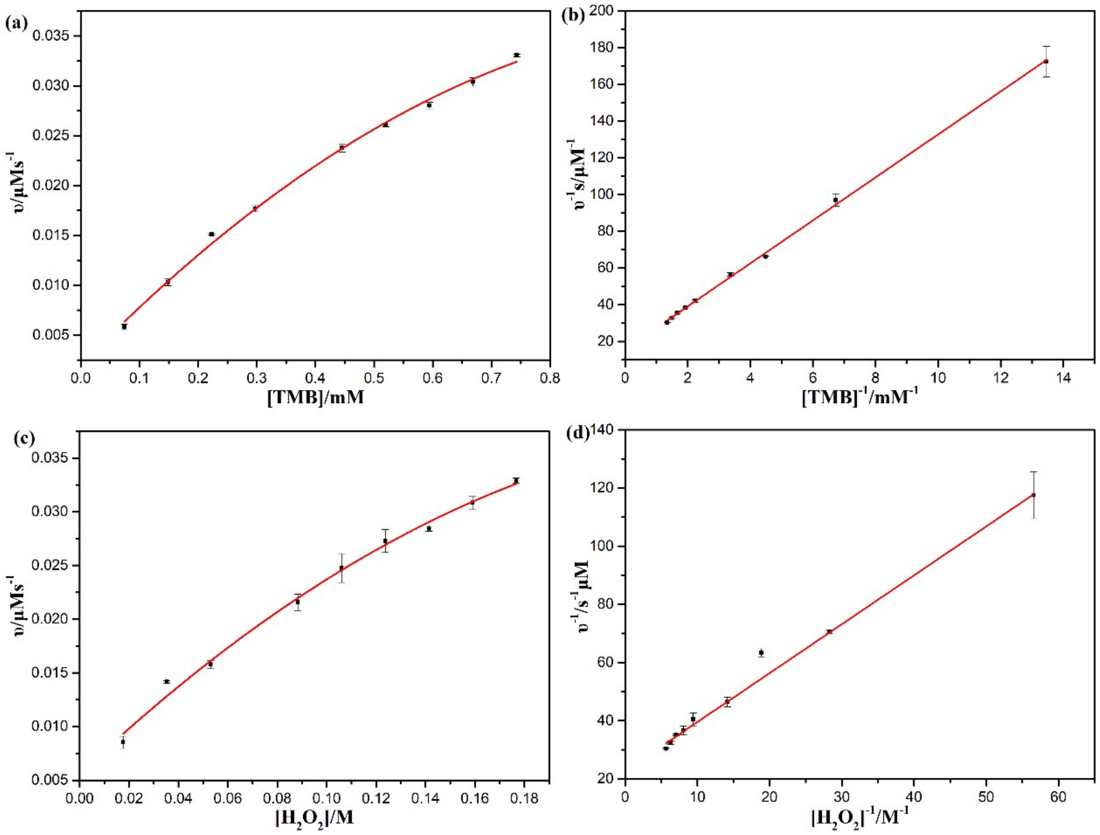

Figure S12. The steady-state kinetic assay and catalytic mechanism of citrate-capped Cu NPs, the initial reaction velocities were measured through the oxidization of TMB in the presence of H_2O_2 at 25℃, 500 μl Hg^{2+}(10 μM), pH 4.0, using 100μl Cu NPs: (a) The H_2O_2 concentration was fixed at 0.177 M and the TMB concentration was varied. (c) The TMB concentration was fixed at 0.743 mM and the H_2O_2 concentration was varied. (b) and (d) were double reciprocal plots of (a) and (c), respectively.

Table S1. Comparisons of the kinetic data of the citrate-capped Cu NPs before and after the addition of Hg^{2+}.

	Substrate	K_m (mM)	V_{max} ($10^{-8}Ms^{-1}$)
Cu NPs	TMB	1.629	4.978
	H_2O_2	83.691	2.469
Cu NPs + Hg^{2+}	TMB	0.742	6.344
	H_2O_2	73.933	4.397

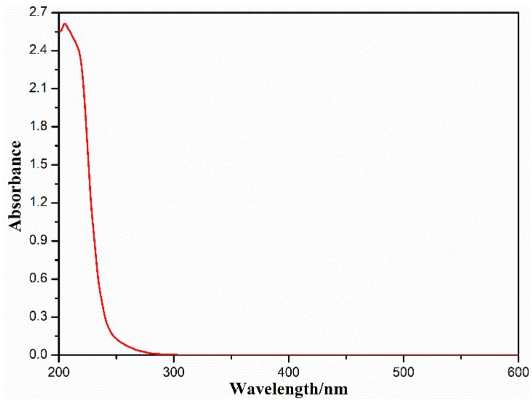

Figure S13. UV-Vis absorption spectra of $CuCl_2$ solution.

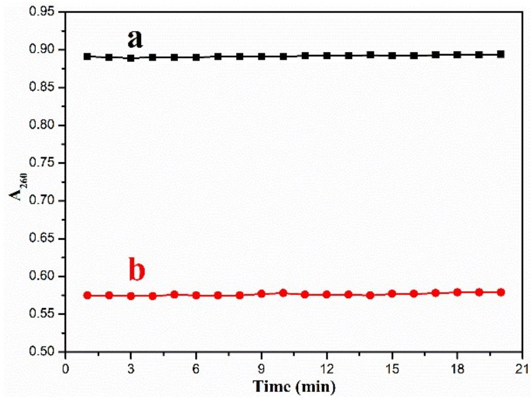

Figure S14. the absorbance values at 260 nm changes over time.(a) 1ml citrate-capped Cu NPs + 1ml H_2O (b)1ml citrate-capped Cu NPs + 1ml Hg^{2+}(3x10^{-6} M). A_{260} represent the absorbance at 260 nm.

Table S2. Determination of Hg^{2+} in real samples based on the peroxidase-like activity of citrate-capped Cu NPs

Spiked (μM)	Detected (μM)	Recovery (%)	RSD (%)	ICP (μM)
0.5	0.53	106.53	1.64	0.48
1	1.16	117.16	2.31	1.03
3	3.22	107.33	2.20	3.20

Table S3. Determination of Hg^{2+} in real samples based on the characteristic absorption peak of citrate-capped Cu NPs

Spiked (μM))	Detected (μM)	Recovery (%)	RSD (%)	ICP (μM)
0.5	0.49	97.98	0.65	0.47
1	0.81	81.07	0.84	0.93
3	2.76	92.00	1.47	2.89

Table S4. Compared of the advantages of two colorimetric methods that proposed in this study.

colorimetric methods	Advantage
Peroxidase-like activity of citrate-capped Cu NPs	high selectivity and sensitivity UV-vis is not strictly necessary, we can prepare test paper for Hg^{2+} detection in the future. (Similar to detecting glucose)[1]
characteristic absorption peak of citrate-capped Cu NPs	high selectivity and sensitivity Don't need TMB-H_2O_2 Chromogenic solution. More convenient The absorbance value at 260nm is time-independent (Fig.S13)

Table S5. Comparison of the different analytical methods for Hg^{2+} sensing

Detection system	method	Linear range/LOD	References
RB-Fe_3O_4@SiO_2	Fluorescence	0-70 μM / 2.13 μM	2
BSA-Au NCs	Fluorescence	0.001-0.020 μM / 0.0005 μM	3
C-DOts	Fluorescence	0-3 μM / 0.0042 μM	4
N-CDs	Fluorescence	0-25 μM / 0.23 μM	5
DNA–Ag/Pt NCs	Colorimetry	0.01-0.20 μM / 0.005 μM	6
BSA-Au NCs	Colorimetry	0.01-10 μM / 0.003 μM	7
Gold NPs	Colorimetry	0.5-50 μM / 0.0185 μM	8
BSA-Pt NCs	Colorimetry	0-0.12 μM / 0.0072μM	9
MoS2 nanosheets	Colorimetry	2-200 μM / 0.5 μM	10
L-cysteine-Cu Nps	Colorimetry	0.5-3.5 μM / 0.043 μM	11
N-lauryltyramine-capped Cu NPs	Colorimetry	0-25 μM / 0.13 μM	12
Citrate- capped Cu NPs	Colorimetry	0.050-10.000 μM / 0.185 μM	This work
	Colorimetry	0.100-6.000 μM / 0.052 μM	This work

References

1. Y. Luo, R. Shen, T. Li, C. Xiong, G. Li and L. Ling, *Talanta*, 2019, **196**, 493-497.
2. Z. Sun, G. Dan, H. Li, Z. Li, Y. Bo and S. Yan, *RSC Adv.*, 2015, **5**, 11000-11008.
3. J. Xie, Y. Zheng and J. Y. Ying, *Chem. Commun.*, 2010, **46**, 961-963.
4. L. Zhou, Y. Lin, Z. Huang, J. Ren and X. Qu, *Chem. Commun.*, 2012, **48**, 1147-1149.
5. R. Zhang and W. Chen, *Biosens. Bioelectron.*, 2014, **55**, 83-90.
6. L.-L. Wu, L.-Y. Wang, Z.-J. Xie, F. Xue and C.-F. Peng, *RSC Adv.*, 2016, **6**, 75384-75389.
7. R. Zhu, Y. Zhou, X.-L. Wang, L.-P. Liang, Y.-J. Long, Q.-L. Wang, H.-J. Zhang, X.-X. Huang and H.-Z. Zheng, *Talanta*, 2013, **117**, 127-132.
8. M. Guo, J. He, S. Ma, X. Sun and M. Zheng, *Nano*, 2017, **12**, 132-142.
9. Z. Dan, C. Chen, L. Lu, Y. Fan and X. Yang, *Sens. Actuator B-Chem.*, 2015, **215**, 437-444.
10. Y. Lu, J. Yu, W. Ye, X. Yao, P. Zhou, H. Zhang, S. Zhao and L. Jia, *Microchimi. Acta*, 2016, **183**, 2481-2489.
11. R. A. Soomro, A. Nafady, Sirajuddin, N. Memon, T. H. Sherazi and N. H. Kalwar, *Talanta*, 2014, **130**, 415-422.
12. S. Megarajan, M. Vidhyalakshmi, K. B. A. Ahmed, V. Murali, B. R. S. Niranjani, N. Saisubramanian and V. Anbazhagan, *RSC Adv.*, 2016, **6**, 87513-87522.